

size until it can no longer exist without collapsing into a small-polaron state.

Finally it is noted that in a discrete (atomic) system both the electron-lattice interaction energy and the strain energy saturate at some maximum value when the electron's radius shrinks smaller than the interatomic separation. One method of incorporating this effect into the continuum model is to disregard the $E(R)$ curve at values of the scaling factor R less than that characteristic of the onset of the saturation effect, R_s . This procedure simply serves to eliminate the small-polaron solution if R_s lies between a maximum and a minimum (at $R = 1$) of $E(R)$. If $R_s > 1$ the solitary solution corresponds to small-polaron formation. In systems with a short-range component of the electron-lattice interaction a change in the physical parameters can produce the abrupt appearance (or disappearance) of small-polaron states (at R_s) in the non-ground-state solution. The energies of such small-polar-

on states are not, however, generally given correctly by this modified continuum model. One does see, in agreement with Refs. 3 and 4 and Shore, Sander, and Kleinman,⁶ that although the nature of the ground state may change abruptly with an alteration of the physical parameters, in the adiabatic limit the ground-state energy does not.

*This work is supported by the U. S. Energy Research and Development Administration and the National Science Foundation (Grant No. GP 21290).

¹H. Fröhlich, Proc. Roy. Soc. London, Ser. A **160**, 230 (1937).

²T. Holstein, Ann. Phys. (N.Y.) **8**, 325 (1959).

³D. Emin, Adv. Phys. **22**, 57 (1973).

⁴Y. Toyozawa, Prog. Theor. Phys. **26**, 29 (1961).

⁵S. I. Pekar, *Untersuchungen Über die Elektronentheorie der Kristalle* (Akademie-Verlag, Berlin, 1954).

⁶H. B. Shore, L. M. Sander, and L. Kleinman, Nature (London) **245**, 44 (1973).

Momentum-Transfer Dependence of the $L_{II, III}$ Edge of $Mg\uparrow$

Susan G. Slusky, P. C. Gibbons, S. E. Schnatterly, and J. R. Fields*
Joseph Henry Laboratories, Princeton University, Princeton, New Jersey 08540
 (Received 20 October 1975)

We report measurements of the $L_{II, III}$ x-ray threshold in Mg at momentum transfers of $q = 0$ and 1.8 \AA^{-1} . We found that a straightforward application of the theory of Mahan, Nozières, and De Dominicis failed to describe the data. We conclude that for Mg, and probably for all polyvalent metals, other effects are at least as important as this theory for describing absorption threshold shapes.

The shapes of soft-x-ray thresholds in simple metals depart from the simple step function expected in the one-electron approximation.¹ Some metals show a peaking at threshold; others do not. Mahan, Nozières, and De Dominicis (MND) formulated a theory to explain these observations.² This many-electron theory describes the effect on threshold shapes of interactions between the core hole and conduction electrons. Peaking is predicted when transitions occur to s partial waves in the conduction band; when transitions to higher partial waves occur, a more rounded threshold shape is predicted, because the screening charge of the core hole is expected to be dominated by s waves. Consequently, when the core is a p state, peaking is predicted, while s core states should have rounded thresholds. These

predictions are in qualitative agreement with soft-x-ray absorption spectra.¹ Inelastic electron scattering can provide a more stringent test of the theory since different conduction-band partial waves can be selected for a given core state by varying the momentum transfer.³ This type of test was first proposed by Doniach, Platzman, and Yue.⁴

The operator causing the transition in electron scattering is $e^{i\vec{q}\cdot\vec{r}}$ where \vec{q} is the momentum transfer and \vec{r} the position operator of an electron in the sample. Since the core state is well localized the transition matrix element can be expanded as

$$\langle\psi_f|1+i\vec{q}\cdot\vec{r}-\frac{1}{2}(\vec{q}\cdot\vec{r})^2+\dots|\psi_i\rangle, \quad (1)$$

where ψ_f and ψ_i are the exact final and initial

states of the system. The expansion is useful when the core radius, a , is smaller than q^{-1} . The first term does not contribute since ψ_f and ψ_i are orthogonal. The second term, which dominates when q is small, causes dipole transitions just as in soft-x-ray absorption. The third term becomes important at larger q values and causes monopole and quadrupole transitions.

In this paper we report measurements of the Mg $L_{II,III}$ threshold. For small q we expect dipole transitions from the $2p$ core state to s waves in the conduction band. At larger q , monopole transitions transfer part of the strength to p waves. Therefore the MND theory predicts a peaked spectrum at $q=0$ and a less sharply peaked spectrum at high q .

More quantitatively, according to the MND theory, the threshold shape can be written

$$S(q, E) \propto \frac{1}{q^4} \sum_{l=0}^{\infty} A_l(q) \left(\frac{\xi}{E - E_T} \right)^{\alpha_l} \theta(E - E_T), \quad (2)$$

where $A_l(q) = |\langle \psi_{f_l} | e^{i\vec{q}\cdot\vec{r}} | \psi_i \rangle|^2$, ψ_{f_l} is the l th partial-wave component of the conduction states near the Fermi energy, ξ is a range parameter expected to be on the order of the Fermi energy, E_T is the threshold energy, α_l is the threshold exponent for partial wave l , and θ is the unit step function. The goal of this work is to determine whether Eq. (2) accurately describes the measured shape of the Mg $L_{II,III}$ threshold for different magnitudes of q using reasonable values of the parameters.

The measurements were carried out on the Princeton University inelastic electron spectrometer described elsewhere.⁵ The beam energy is 300 keV; the energy and momentum resolutions in this experiment were 0.088 eV and 0.3 \AA^{-1} , respectively. Two complete sets of data were taken in the energy range 48.4–51.2 eV and at momentum transfers of $q=0$ and 1.8 \AA^{-1} . Typical counting rates were 27 000 and 250 counts per second at $q=0$ and 1.8 \AA^{-1} , respectively. Repeated scans were taken to improve the statistics. The total number of counts per point was 439 000 at $q=0$ and 299 000 at $q=1.8 \text{ \AA}^{-1}$. The edge height was 40% of the total counting rate at $q=0$, and 14% at $q=1.8 \text{ \AA}^{-1}$. Samples of about 10^3 \AA thickness were made by subliming Mg in the baked vacuum chamber onto carbon substrates. The pressure after sample deposition was several nanoTorr. The threshold shape remained unchanged during 3 days of data taking despite noticeable degradation of surface excitations.

A straight line was fitted to the spectra below threshold and subtracted from the spectra to yield the curves in Fig. 1. To fit the measured spectra with the theoretical shape of Eq. (2), the theoretical shape, with a given set of parameters, was convoluted first with the derivative of a Fermi function to account for finite temperature, then with a Gaussian of standard deviation Γ to account for finite lifetime and spectrometer energy resolution. Two such curves with amplitude ratio S and energy difference Δ were added together to represent the spin-orbit splitting of the $2p$ core state.

Using the $q=0$ data, the following parameters were adjusted to minimize χ^2 : E_T , Δ , S , Γ , and α_0 . The ratio $A_2(0)/A_0(0)$ was 0.15 as calculated by Smith⁶ and α_2 was fixed at -0.1 . The values of the other parameters were found to be insensitive to α_2 , so it was not varied. The range parameter, ξ , was taken to be the Fermi energy, 7.13 eV. Because of the method of normalizing the data, the results are insensitive to this value. The agreement between the computed and measured spectra was found to be very sensitive to the first four of the above parameters in the leading-edge area, whereas it was most sensitive to α_0 beyond threshold. The theoretical shape was normalized to the data 0.5–0.7 eV above the higher-energy threshold. The solid line in Fig. 1 shows the theoretical shape obtained this way for the $q=0$ spectrum.

The parameters determined from the $q=0$ data are the $p_{1/2}$ threshold energy $E_T = 49.87 \pm 0.01$ eV,

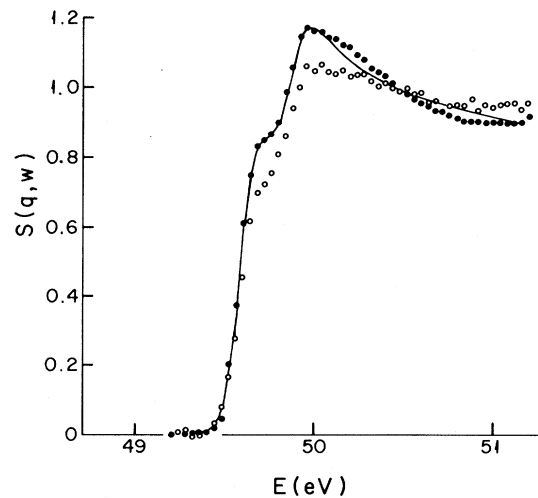


FIG. 1. Normalized data, after background subtraction. Dots, $q=0$; open circles, $q=1.8 \text{ \AA}^{-1}$; line, $q=0$ theory as described in the text.

the spin-orbit splitting $\Delta = 0.28 \pm 0.01$ eV, the ratio of $p_{3/2}$ to $p_{1/2}$ strength $S = 1.86 \pm 0.05$, $\Gamma = 0.06 \pm 0.01$ eV, and $\alpha_0 = 0.18 \pm 0.005$. The uncertainty in E_T was determined by the observed slow variation in the spectrometer zero of energy. The precision in the value of Δ was limited by the finite grid size used in the computer program. The uncertainties in S , Γ , and α_0 are statistical and indicate the change in that parameter which increases the unreduced χ^2 by 1, leaving all other parameters fixed. These statistical uncertainties do not include systematic errors or correlations between the parameters.

We then formed the difference spectrum between the $q=0$ and $q=1.8 \text{ \AA}^{-1}$ data by normalizing both sets of data 0.5–0.7 eV above E_T and subtracting one from the other point by point. The spectral changes which must be explained are most easily apparent in this difference curve. Except for the region immediately above threshold, the difference curve is small and relatively featureless out to 60 eV.

The difference curve was corrected for thermal-diffuse, multiple scattering in which an electron scatters elastically from disorder in

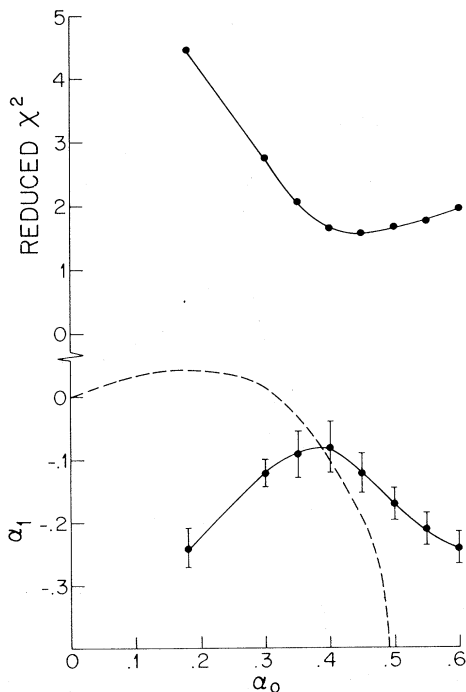


FIG. 2. Fitted α_1 for trial values of α_0 , and reduced χ^2 for each fit, using the difference curve shown in Fig. 3. The solid lines are intended only to guide the eye. The dashed line is the improved compatibility relation of Dow and Robinson (Ref. 6).

the sample with $q=1.8 \text{ \AA}^{-1}$ and then scatters causing a core excitation with $q=0$. This has the effect of adding to the 1.8-\AA^{-1} raw data some of the $q=0$ shape. By studying the easily apparent, thermal diffuse contribution to the Mg plasmon spectrum we found that such double scattering accounted for $(23 \pm 5)\%$ of the $q=1.8 \text{ \AA}^{-1}$ spectrum and corrected the difference curve accordingly.

Using the parameters described above and $A_1(1.8)/A_0(1.8) = 0.74$ as calculated by Smith,⁶ we formed a theoretical difference curve in the same way as the experimental one and varied α_1 to minimize χ^2 . The result was a very poor fit (reduced $\chi^2 = 4.5$) and $\alpha_1 = -0.24$. This value of α_1 , with $\alpha_0 = 0.18$, does not satisfy the Friedel sum rule, giving too little screening charge by an order of magnitude.

We found two ways in which modified parameter values would describe our measured difference curve. First, by allowing the ratio $A_1(1.8)/A_0(1.8)$ to increase to at least 4, the resulting α_1 increased to acceptable values. We reject this alternative; there should be little ambiguity in the value of this ratio.⁶ Second, by allowing α_0 to increase, acceptable values of α_1 could be achieved with smaller values of χ^2 . Figure 2 shows a plot of the best α_1 and the associated χ^2 versus α_0 . The dashed line is the improved compatibility relation of Dow and Robinson.⁷ Only one point on our curve of α_1 versus α_0 can satisfy the Friedel sum rule; that point is given by the intersection of our curve with that of Dow and Robinson. The vertical error bars indicate the change in α_1 needed to increase the unreduced χ^2 by 2. Figure 3 shows the experimental differ-

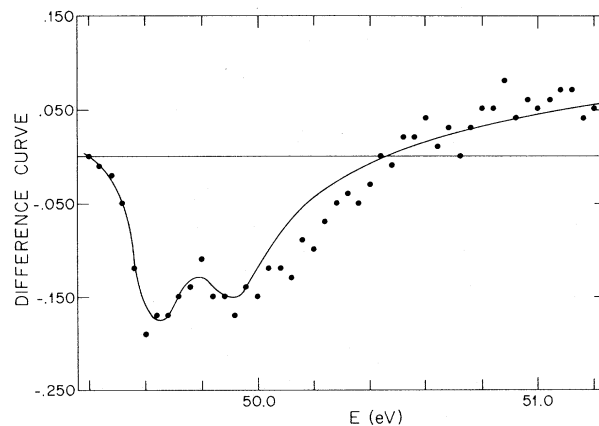


FIG. 3. Dots, difference curve obtained by subtracting the two data sets shown in Fig. 1. Solid line, theoretical difference curve described in the text.

ence curve, and the theoretical result for $\alpha_0 = 0.40$ and $\alpha_1 = -0.08$.

Clearly, our difference curve requires larger values of α_0 than the $q=0$ spectrum. This could be due either to structure in the one-electron density of states, or to the inapplicability of the MND theory to this problem. In addition, note that our measured $q=0$ spectrum is linearly decreasing above threshold while the theoretical shape is concave upwards. The difference curve, Fig. 3, also shows a systematic deviation from the theoretical shape in the same region.

Haensel *et al.*⁸ found $E_T = 49.87 \pm 0.1$ eV and $\Delta = 0.27$ eV. To our knowledge no one has previously reported a value for S . The ideal small- Z LS coupling value is $S=2$. Our value of Γ implies a full width at half-maximum of the broadening function of 0.141 eV, while our measured machine resolution is 0.088 eV. The extra broadening could be due to the finite lifetime of the core hole. Dow and Sonntag have analyzed the photoabsorption shape of Haensel *et al.*, and, fitting it with the MND theory, find $\alpha_0 = 0.18 \pm 0.04$ in excellent agreement with our result for the $q=0$ spectrum.⁹ Neddermeyer has analyzed his Mg x-ray emission measurements to obtain $\alpha_0 = 0.3 \pm 0.07$.¹⁰ Absorption and emission exponents should agree according to the MND theory. The discrepancy between this value of α_0 and the absorption and electron scattering values is consistent with the one-electron density of states playing an important role in determining the threshold shape. If the one-electron density of states varies rapidly with energy near the Fermi energy due to band structure, for example, then exponents α_i fitted to absorption and emission data need not agree.

Measurements of the asymmetry of x-ray-photoemission-spectroscopy lines yield a value of $\alpha_\infty = 0.13 \pm 0.01$.¹¹ Precise determination of α_0 from this α_∞ does not appear possible, using either a two-phase-shift model¹¹ or the improved compatibility relation of Dow and Robinson.¹²

The MND theory alone cannot account for both the $q=0$ shape and our difference curve. The exponents which fit the two curves are different. Is this due to a failure of the MND theory or to the influence of one-electron effects? If it is due to one-electron effects, the problem is to combine them with the MND theory. This problem has not been solved theoretically.¹ The values of exponents derived from our difference curve (Fig. 2) are correct if one assumes a q -independent, additive, one-electron-density-of-states

contribution to the spectrum. Many-electron and one-electron effects are more realistically described as multiplicative. We found, however, that no q -independent multiplicative one-electron density of states can describe our difference curve, for any pair of exponents (α_0, α_1) satisfying the compatibility relationship. If we allow either a multiplicative or an additive one-electron density of states to vary with q , then the problem of fitting MND exponents becomes indeterminate.

Our results call into question all determinations of soft-x-ray threshold exponents in polyvalent metals based on emission, absorption, or electron scattering measurements of edge shapes, because these determinations were made neglecting one-electron effects. Accurate calculations of transition strengths for various partial waves would allow us to include one-electron density-of-states effects and might result in accurate threshold exponents. The general disagreement between emission and absorption shapes in polyvalent metals may be due to such one-electron effects caused by band structure. It is disturbing, however, that there appears to be a similar discrepancy in sodium, for which band-structure effects should not be so important.¹

We are grateful to Professor J. D. Dow for extensive fruitful telecommunications on this subject.

†Work supported by the National Science Foundation under Grant No. DMR74-16337.

*Present address: Department of Biophysics, Johns Hopkins University, Baltimore, Md. 21218.

¹G. D. Mahan, in *Solid State Physics*, edited by H. Ehrenreich, F. Seitz, and D. Turnbull (Academic, New York, 1974), Vol. 29, p. 75.

²G. D. Mahan, *Phys. Rev.* **163**, 612 (1967); P. Nozières and C. T. De Dominicis, *Phys. Rev.* **178**, 1097 (1969).

³J. J. Ritsko, S. E. Schnatterly, and P. C. Gibbons, *Phys. Rev. B* **10**, 5017 (1974).

⁴S. Doniach, P. M. Platzman, and J. T. Yue, *Phys. Rev. B* **4**, 3345 (1971).

⁵P. C. Gibbons, J. J. Ritsko, and S. E. Schnatterly, to be published.

⁶D. L. Smith, thesis, University of Illinois, 1974 (unpublished).

⁷J. D. Dow and J. E. Robinson, to be published.

⁸R. Haensel *et al.*, *Phys. Status Solidi* **2**, 85 (1970).

⁹J. D. Dow and B. F. Sonntag, *Phys. Rev. Lett.* **31**, 1461 (1973).

¹⁰H. Neddermeyer, in *Proceedings of the Fourth International Conference on Vacuum Ultraviolet Radiation Physics, Hamburg, 1974*, edited by E. E. Koch,

R. Haensel, and C. Kunz (Pergamon, New York, 1974), p. 665.

¹¹L. Ley *et al.*, Phys. Rev. B **11**, 600 (1975); P. H.

Citrin, G. K. Wertheim, and Y. Baer, Phys. Rev. Lett. **35**, 885 (1975).

¹²J. D. Dow, private communication.

Measurement of ⁴³Ca-¹⁹F Dipolar Energy in Antiferromagnetic CaF₂

M. Goldman and J. F. Jacquinot

*Service de Physique du Solide et de Résonance Magnétique, Centre d'Etudes Nucléaires de Saclay,
91190 Gif-sur-Yvette, France*

(Received 8 December 1975)

We have measured the ⁴³Ca-¹⁹F dipolar energy in CaF₂, as deduced from the first moment of the ⁴³Ca resonance signal, as a function of the fluorine-fluorine energy. The Ca-F energy, which depends on the local longitudinal susceptibility of the fluorine spins, is theoretically expected to peak at the paramagnetic-antiferromagnetic transition. Such a peak is indeed observed.

Magnetic ordering can be produced in nuclear spin systems subjected to dipolar interactions by cooling them below 1 μ K. The principles of production and of study of nuclear magnetic ordering, as well as experimental evidence for nuclear ferromagnetism and antiferromagnetism, have been reported in a number of articles.¹⁻⁶

The cooling concerns only the nuclear spins. It is performed in a two-step process: dynamic polarization in high field, followed by nuclear adiabatic demagnetization. When the adiabatic demagnetization is performed in the rotating frame (i.e., it consists of a fast passage stopped at resonance), the final-spin Hamiltonian is the familiar truncated, or secular, dipole-dipole Hamiltonian \mathcal{H}_D' ; it depends on the orientation of the external field H_0 with respect to the crystal-line axes. The ordering produced by adiabatic demagnetization depends also on that orientation, as well as on the sign of the spin temperature, positive or negative.

In particular, in a simple cubic system of spins $\frac{1}{2}$, when the demagnetization in the rotating frame is performed at negative temperature with H_0 parallel to a fourfold axis, theory predicts the occurrence of an antiferromagnetic structure in which the nuclear planes perpendicular to H_0 carry magnetizations alternately parallel and antiparallel to H_0 . This structure has been produced and studied on the ¹⁹F system in spherical samples of CaF₂. The occurrence of antiferromagnetism was inferred from the characteristic variations of the longitudinal and transverse susceptibilities as a function of entropy or energy: Below the transition, χ_{\perp} remains constant, whereas χ_{\parallel} decreases slightly. The change in the behavior of

these quantities when going from paramagnetism to antiferromagnetism is smooth, and no marked singularity is observed, nor expected, at the transition.

In the present work we have studied, for the same structure, the local longitudinal susceptibility of the fluorine spins as probed by the resonance signal of the low-abundance ⁴³Ca isotope, a phenomenon exhibiting a marked critical behavior.

When the ¹⁹F spins are demagnetized, the shape of the resonance signal of the unpolarized ⁴³Ca is that of the derivative of a bell-shaped curve. This is the well-known signal for adiabatic demagnetization in the rotating frame.⁷ In the present case when the ⁴³Ca (the spins S) are much less abundant than the ¹⁹F (the spins I), $N_S/N_I \approx 6.5 \times 10^{-4}$, this signal can be given the following simple physical interpretation. Each spin S is treated independently. A given spin S in a state $S_z = m$ creates a dipolar field at the sites of the nearby spins I . Through flip-flop processes, the latter acquire polarizations departing slightly from their normal equilibrium values. These departures are inhomogeneous in space and proportional to m , in the linear approximation. They create at the site of the spin S a dipolar field proportional to m , which shifts the resonance frequency of that spin. Spins S with opposite values of m experience opposite resonance shifts. Since, furthermore, spins S with $m < 0$ give an absorption signal and spins S with $m > 0$ an emission signal, we observe a signal shaped like that of the derivative of a bell-shaped curve, which reflects the local susceptibility of the spins I to the dipolar field of the spins S .